J. Fluid Mech. (1986), *vol.* 165, *pp.* 61–71
Printed in Great Britain

Force on a circular cylinder in viscous oscillatory flow at low Keulegan–Carpenter numbers

By TURGUT SARPKAYA

Mechanical Engineering, Naval Postgraduate School, Monterey, California 93943, USA

(Received 12 August 1985)

This paper presents the in-line force coefficients for circular cylinders in planar oscillatory flows of small amplitude. The results are compared with the theoretical predictions of Stokes (1851) and Wang (1968). For two-dimensional, attached- and laminar-flow conditions the data are, as expected, in good agreement with the Stokes–Wang analysis. The oscillatory viscous flow becomes unstable to axially periodic vortices above a critical Keulegan–Carpenter number K ($K = U_m T/D$, U_m = the maximum velocity in a cycle, T = the period of flow oscillation, and D = the diameter of the circular cylinder) for a given β ($\beta = Re/K = D^2/\nu T$, $Re = U_m D/\nu$, and ν = the kinematic viscosity of fluid) as shown experimentally by Honji (1981) and theoretically by Hall (1984). The present investigation has shown that the Keulegan–Carpenter number at which the drag coefficient C_d deviates rather abruptly from the Stokes–Wang prediction nearly corresponds to the critical K at which the vortical instability occurs.

1. Introduction

Sinusoidally oscillating flow about a cylinder or the sinusoidal motion of a cylinder in a viscous fluid otherwise at rest has long been of special interest to fluid dynamicists and offshore engineers (see e.g. Keulegan & Carpenter 1958; Sarpkaya 1976, 1977; Bearman *et al.* 1985). The in-line force acting on the cylinder is assumed to be given by a linear sum of the drag and inertial forces per unit length as

$$F = \tfrac{1}{2}\rho D C_d |U| U + \tfrac{1}{4}\pi\rho D^2 C_m \frac{dU}{dt}, \tag{1}$$

in which ρ is the density of fluid, D the diameter of the circular cylinder, U the velocity of the ambient flow ($U = U_m \cos\theta$ with $\theta = 2\pi t/T$), T the period of flow oscillation, and t the time. C_d and C_m represent the drag and inertia coefficients, to be determined experimentally through the use of the method of least squares or Fourier averaging over a cycle (see e.g. Keulegan & Carpenter 1958; Sarpkaya & Isaacson 1981). Equation (1) is known as the Morison equation. It will be referred to hereafter as the MOJS equation to recognize the joint contributions of its originators (Morison, O'Brien, Johnson and Schaaf 1950). Equation (1) was proposed as an approximate solution to a complex problem. Its justification is strictly pragmatic and rests with experimental confirmation.

A great deal of experimental effort has been devoted during the past decade to the determination of the drag and inertia coefficients, particularly for smooth and rough circular cylinders, in terms of the Keulegan–Carpenter number ($K = U_m T/D$), Reynolds number ($Re = U_m D/\nu$) or $\beta (= D^2/\nu T)$, and the relative roughness k/D

(Sarpkaya 1976; Sarpkaya & Isaacson 1981, where numerous additional references may be found). The analytical efforts, based largely on some form of the shear-layer discretization, have not been successful in predicting the characteristics of sinusoidally oscillating separated flow primarily because there does not yet exist a sound method for the determination of the position of the separation points on a circular cylinder in a time-dependent turbulent boundary-layer flow.

Practically all the laboratory and ocean-based experiments have been conducted for K larger than about 4 and it is assumed that C_d for $K < 4$ is unimportant and C_m has the theoretical potential-flow value of the body shape tested. These assumptions miss a number of interesting flow phenomena and ignore the possibility that for large two- or three-dimensional bodies near the ocean bottom (small K and large Re) C_d may be quite large and the actual value of C_m may exceed its ideal value.

Stokes (1851) was the first to show that the force acting on a cylinder or sphere oscillating sinusoidally in a viscous fluid is dependent on both K and Re (or β). In the case of a *fixed* circular cylinder in a sinusoidally oscillating flow Stokes force may be expressed in terms of the MOJS equation by noting that over a flow cycle $|\cos\theta|\cos\theta$ may be approximated by $(8/3\pi)\cos\theta$. Then one has (see also Rosenhead 1963, p. 392)

$$C_d = \frac{3\pi^3}{2K}[(\pi\beta)^{-\frac{1}{2}} + (\pi\beta)^{-1} + O(\pi\beta)^{-\frac{3}{2}}] \tag{2}$$

and

$$C_m = 2 + 4(\pi\beta)^{-\frac{1}{2}} + O(\pi\beta)^{-\frac{3}{2}}. \tag{3}$$

Equations (2) and (3) are valid only for large values of β. Wang (1968) extended this analysis to $O[(\pi\beta)^{-\frac{3}{2}}]$ using the method of inner and outer expansions. His solution, valid for $K \ll 1$, $Re\,K \ll 1$, and $\beta \gg 1$, may be reduced to

$$C_d = \frac{3\pi^3}{2K}[(\pi\beta)^{-\frac{1}{2}} + (\pi\beta)^{-1} - \tfrac{1}{4}(\pi\beta)^{-\frac{3}{2}}] \tag{4}$$

and

$$C_m = 2 + 4(\pi\beta)^{-\frac{1}{2}} + (\pi\beta)^{-\frac{3}{2}}. \tag{5}$$

The expressions (4) and (5) differ from (2) and (3) only in the last terms. Stokes and Wang's solutions yield virtually identical results in the range of their validity, i.e. for large β.

Relatively few experiments have been carried out with sinusoidally oscillating cylinders at low Keulegan–Carpenter numbers. Honji (1981) oscillated a circular cylinder in water at rest in the range of $70 < \beta < 700$ and $0 < K < 4$ and investigated the stability of the flow. He has delineated three regions in the (K, β)-plane: a region (corresponding to relatively small K) in which no 'streaks' formed because the flow remained attached, stable and two-dimensional; a second region in which the flow became unstable to axially periodic vortices ('equally spaced horizontal streaks of chains of separated dye sheets, each in a form like a mushroom'); and a third region in which no clear streaks formed because the flow became turbulent 'due to long standing separation'. Honji attributed the instability in the second region to centrifugal forces.

Subsequently, Hall (1984) carried out a stability analysis of that flow, valid only in the limit $\beta \to \infty$ and $K \to 0$, and showed that 'oscillatory viscous flows interacting with rigid boundaries of convex curvature can become unstable to Taylor–Görtler vortices'. His analysis validated Honji's data.

Hall's critical Keulegan–Carpenter number may be written as

$$K_{cr} = Re_{cr}/\beta = 5.778\beta^{-\frac{1}{2}}(1+0.205\beta^{-\frac{1}{4}}+\ldots), \tag{6}$$

according to which the critical Reynolds number Re_{cr} increases with increasing β (e.g., $Re_{cr} = 6433$, $K_{cr} = 0.57$ for $\beta = 11240$).

Bearman *et al.* (1985) reported experimental data and analysis for a number of cylinders of different cross-section including circular cylinders and sharp-edged sections in planar oscillatory flows of small amplitude. Their maximum β for the circular cylinders was 1665. They have concluded that the experimental values of C_d are in approximate agreement with Wang's predictions below a given value of K_s '(depending on the β parameter, but somewhere in the region of 2)'. They have attributed the increase in C_d for $K > K_s$ to the onset of flow separation and vortex shedding, thereby suggesting that the laminar-flow analysis of Wang (1968) is valid up to the onset of laminar separation. Their C_m data agreed fairly well with that given by (5) for $K < K_s$. Bearman *et al.*'s data did not permit them to make a connection between the Stokes–Wang analysis, Honji's data and Hall's stability analysis.

The present paper presents in-line force data for one rough and three smooth cylinders over a large range of β with measurements carried out in oscillatory flow in a U-shaped water tunnel. The original aim of the investigation was to provide data and to check the validity of the Stokes–Wang analysis. However, the experiments provided information beyond the original objectives and helped to establish a connection between the variation of C_d, inception of the vortical instability, boundary-layer transition, and flow separation.

2. Experimental arrangement and presentation of results

Force measurements were carried out in a U-shaped oscillating-flow tunnel. It is 6.7 m high and has a 10.7 m long horizontal test section of 0.92 m width and 1.45 m height. Purely sinusoidal oscillations can be maintained indefinitely at the desired amplitude. For this purpose the output of a 1 hp fan is connected to the top of one of the legs of the tunnel through a 1 m diameter pipe. A butterfly valve between the top of the tunnel and the supply line oscillates sinusoidally at the natural period of water oscillations in the tunnel (5.3525 s), synchronized with the water oscillation by using an electronic feedback control system. The amplitude of the oscillations is varied by constricting or enlarging an orifice at the exit of the fan. The amplitude of the oscillations is measured both by a differential pressure transducer and two capacitance gauges.

Each cylinder was 0.92 m long and mounted horizontally, being supported at each end on specially designed load cells. The ends of the test cylinder were closed and a gap of about 0.5 mm was provided between the ends and the tunnel walls. The unfiltered in-line force and flow oscillation signals were recorded simultaneously in digitized form (720 points per cycle per signal) through the use of an A/D converter. The Fourier-averaged drag and inertia coefficients were calculated from the average of 50 cycles of data. Experiments for a given cylinder were repeated at least three times on different days. Cylinders of various diameters were used to achieve the desired β values.

The drag and inertia coefficients for smooth cylinders are presented in figures 1 ($\beta = 1035$), 2 ($\beta = 1380$), and 3 ($\beta = 11240$) as a function of K. Figure 4 shows the force coefficients for a sand-roughened cylinder ($k/D = \frac{1}{100}$ and $\beta = 1800$). Another important characteristic of the calculated and measured in-line forces, normalized

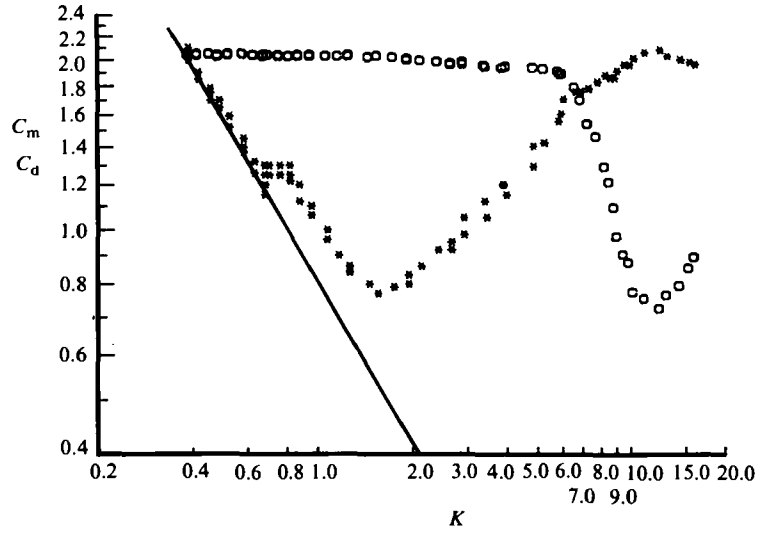

FIGURE 1. Drag and inertia coefficients *vs* Keulegan–Carpenter number. Experiment: ○, C_m; *, C_d; theory, —— (all for $\beta = 1035$).

with respect to $0.5\rho DU_m^2$, is their root-mean-square values, which may be shown, through the use of the MOJS equation, to reduce to (Sarpkaya 1976)†

$$C_f(\text{r.m.s.}) = \left(\tfrac{3}{8}C_d^2 + \frac{\pi^4 C_m^2}{2K^2}\right)^{\frac{1}{2}}. \tag{7}$$

Figure 5 shows the experimental values of C_f(r.m.s.) as a function of K. Equation (7) shows that C_f(r.m.s.) approaches its inviscid value of $\sqrt{(2)}\,\pi^2/K$ for large β (i.e. for $C_d = 0$ and $C_m = 2$). The experimental data fall on this asymptotic theoretical line (except for K larger than about 9). This is entirely expected since the second term in (7) dominates C_f(r.m.s.), i.e. the flow is in the inertia-dominated regime.

Flow-visualization studies were carried out in a glass-sided water tank of 62 cm high, 244 cm long and 122 cm wide. Three smooth cylinders of $D = 2.54$ cm ($L/D = 24$), 5.08 cm ($L/D = 12$) and 7.7 cm ($L/D = 6.85$) and one sand-roughened cylinder ($D = 5.08$ cm, $k/D = \frac{1}{100}$) were oscillated sinusoidally by means of a slider-crank mechanism. The apparatus and the method of flow visualization (electrolytic precipitation from a thin strip of solder) were nearly identical with those used by Honji (1981). The cylinders were held in a vertical position. There was a gap of about 1 mm between the end of the cylinder and the glass bottom of the water tank. The solder strips were about 2 mm wide. The cylinder surface and the solder strips were roughened with sand, which was sieved and uniformly applied on the cylinder surface with an air-drying epoxy paint (for additional details see Sarpkaya 1976). A thin layer of oil was spread over the free surface to prevent evaporation cooling and thereby minimize convection currents. Figure 6 is a sample picture of the streaked flow along the cylinder ($K = 1.1$, $\beta = 1380$). The streaks are nearly equally spaced along the cylinder (about 0.6–0.7 D). The vortex sheets forming on the cylinder on each side of the streak wrap up into a pair of vortices of opposite sign,

† Note that there is a printing error in Bearman *et al.*'s (1985) equation (6) corresponding to our equation (7).

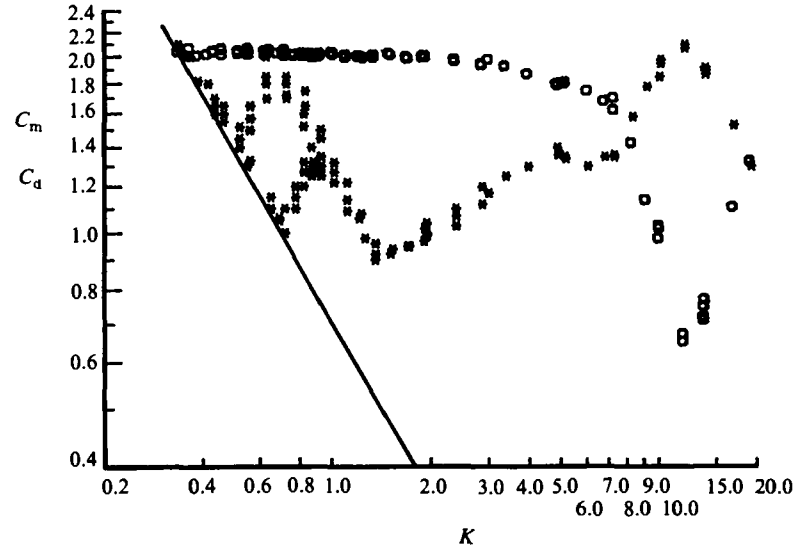

FIGURE 2. Drag and inertia coefficients *vs* Keulegan–Carpenter number. Experiment: ○, C_m; *, C_d; theory, —— (all for $\beta = 1380$).

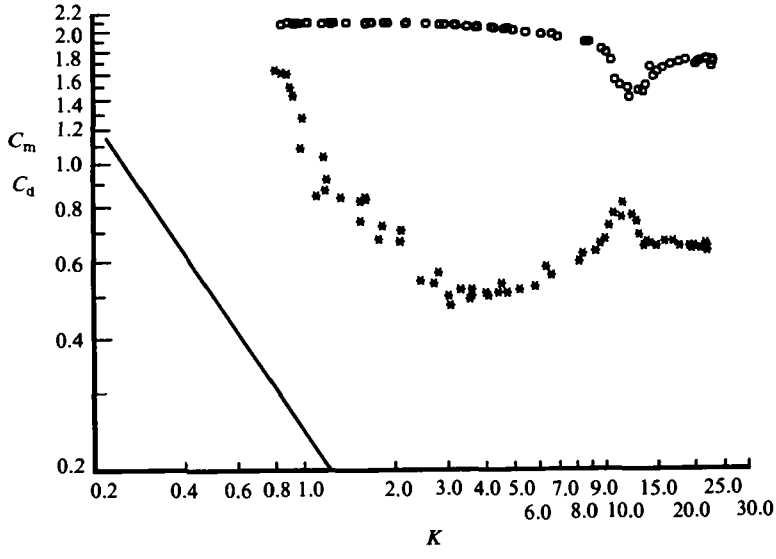

FIGURE 3. Drag and inertia coefficients *vs* Keulegan–Carpenter number. Experiment: ○, C_m; *, C_d; theory, —— (all for $\beta = 11240$).

giving the streak a mushroom-shaped cross-section. The roll-up of the vortex sheets is known to be accompanied by Helmholtz instability which produces turbulence. It was not possible to observe Helmholtz instability in the present tests owing to a number of difficulties associated with the size of the streaks.

Honji (1981) did not give a name to the vortical instability and noted that it 'seems to be a kind of centrifugal one'. Hall (1984) called it the 'Taylor–Görtler instability' and referred to the streaks as the 'Taylor–Görtler cells'. The original Görtler instability involved laminar flow on a concave surface and gave wavelengths of the

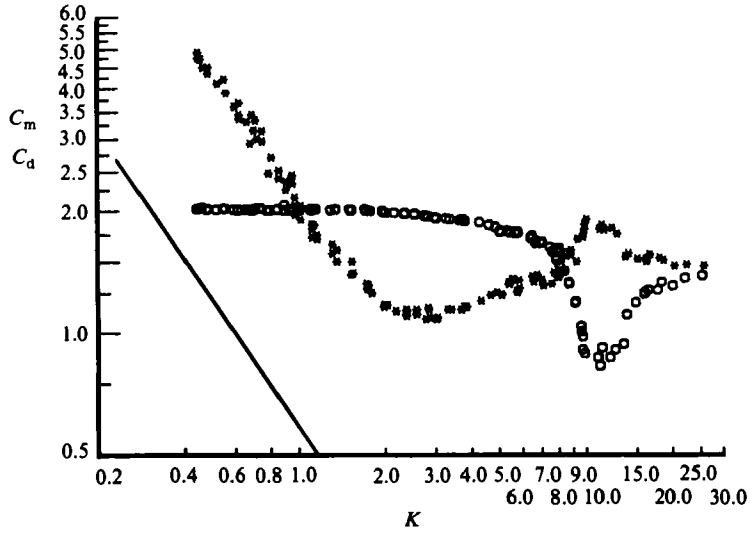

FIGURE 4. Drag and inertia coefficients for a rough cylinder *vs* Keulegan–Carpenter number. Experiment: ○, C_m; *, C_d; theory, —— (all for $k/D = \frac{1}{100}$ and $\beta = 1800$).

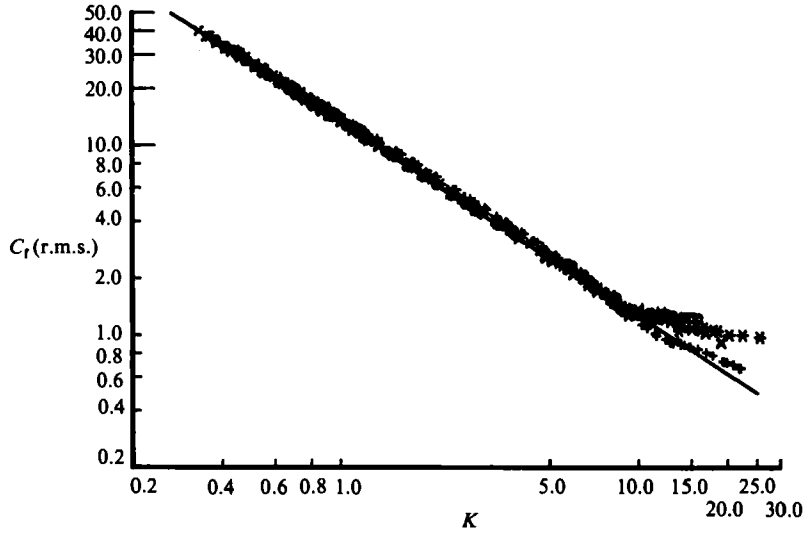

FIGURE 5. Root-mean-square value of the in-line force coefficient *vs* Keulegan–Carpenter number. Experiment: ○, $\beta = 1035$; *, $\beta = 1380$; ×, $\beta = 1800$ $(k/D = \frac{1}{100})$; +, $\beta = 11240$; theory $(C_f(\text{r.m.s.}) = \sqrt{2}\,\pi^2/K)$.

order of the boundary-layer thickness in steady flow. The instability associated with the flow on a cylinder oscillating transversely in a fluid at rest is of the order of the cylinder diameter. Furthermore, it is subcritical in nature, as noted by Hall. In the Taylor problem the bifurcation to a Taylor-vortex flow is almost invariably supercritical. Thus, it appears that it is probably not appropriate to call the streaked flow under consideration the Taylor–Görtler instability in spite of a number of similarities. It may be called 'Honji instability', vortical instability, or the instability of the steady streaming boundary-layer flow.

Honji's data, Hall's prediction [(6)] and the present data are shown in figure 7. The

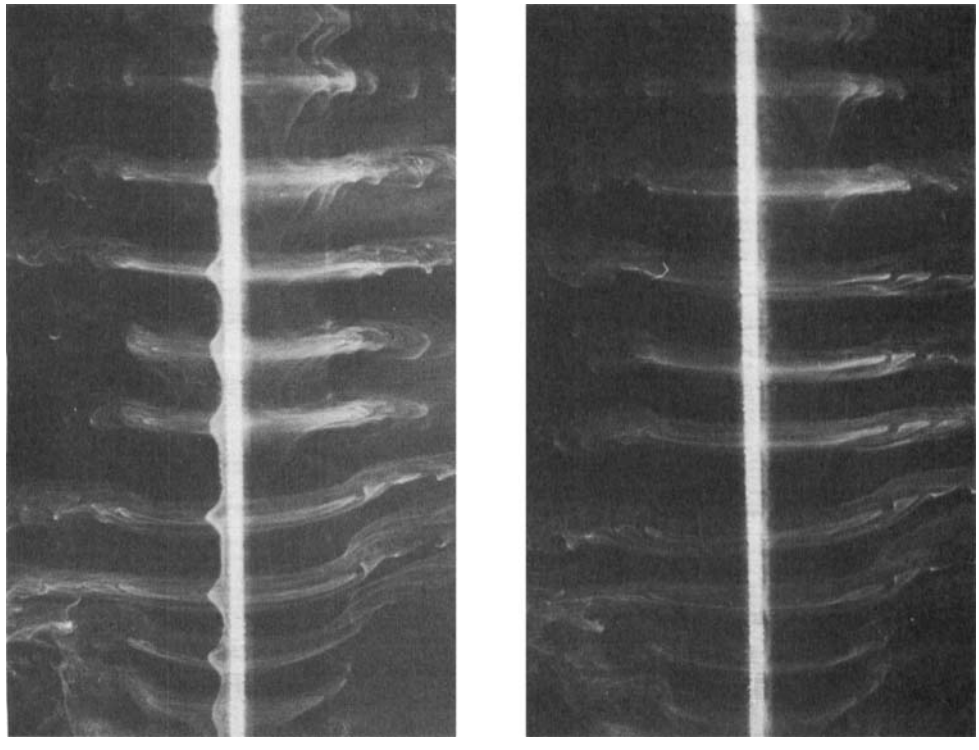

FIGURE 6. Formation of mushroom-shaped vortices (Honji instability) on a smooth cylinder. Direction of cylinder oscillation is parallel to this page. Left: $2\pi t/T = 100°$; Right: $2\pi t/T = 90°$ (both for $K = 1.1$ and $\beta = 1380$).

upper data points (symbols $\times$) denote transition to turbulence over the smooth cylinder. These points exhibit larger scatter due to the fact that the observation of transition is somewhat subjective. Also shown in figure 7 is the mean line through the data points at which separation was observed to occur on smooth cylinders. It must be emphasized that the determination of the onset of separation is just as subjective as that of transition due to a number of difficulties associated with the flow visualization. If the voltage applied between the solder strip and the electrode is kept below 5 volts, the white smoke (a metallic compound) is rather weak and its separation from the cylinder surface is not easy to see. If the voltage is increased to 10 volts, the white smoke becomes quite strong and clearly visible. However, the observations must be made rather quickly (in about 5 min) since the metallic compound (slightly heavier than water) begins to roll downwards along the cylinder surface and gives rise to complex three-dimensional streak sheets. In spite of these difficulties it was possible to delineate fairly accurately whether the separation preceded or followed the transition.

The flow-visualization experiments with the rough cylinder were considerably more difficult partly due to the onset of instability at relatively smaller K, partly due to the diffusion of the metallic smoke by the time it reached the separation points and partly because the K values at which separation occurred were considerably higher than those for the smooth cylinder. It is because of these difficulties that the efforts were concentrated on one particular value of β. Repeated tests with $\beta = 1800$ yielded $K_{cr} = 0.40$, $K_t = 1.1$ (onset of turbulence), and $K_s = 2$ (separation).

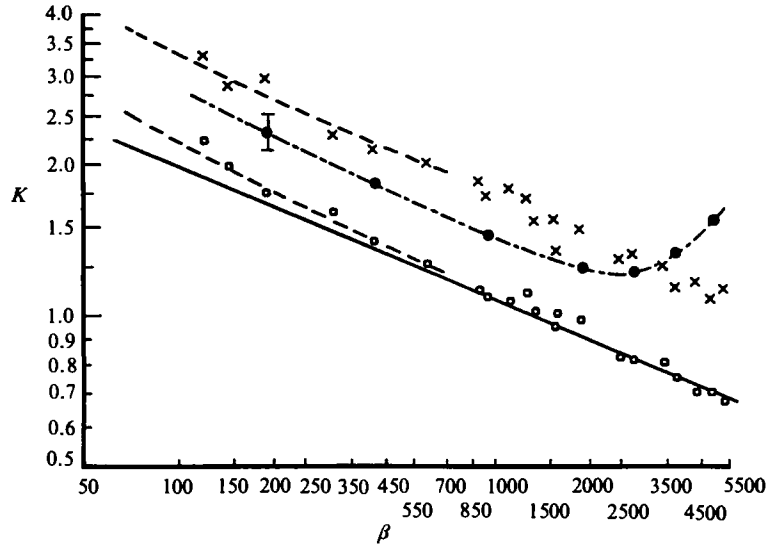

FIGURE 7. Inception of Honji instability, separation and turbulence on an oscillating cylinder. Experiment: ○, Honji instability; ●, separation; ×, turbulence; – – – –, mean line through Honji's data (lower line: Honji instability, upper line: turbulence). Theory: ——, Hall.

3. Discussion of results

Figure 1 shows four broad regimes of flow: (i) $0 < K < K_{cr}$ ($K_{cr} \approx 0.75$ for $\beta = 1035$), referred to hereafter as the Stokes–Wang regime, where the laminar flow is attached and stable; (ii) $K_{cr} < K < K_{md}$ ($K_{md} \approx 1.6$ for $\beta = 1035$), where the laminar flow becomes unstable to axially periodic vortices, which eventually leads to separation, turbulence and minimum C_d. It must be emphasized that here the term 'eventually' refers to a change taking place with increase of the parameter K. Thus, there exists a flow regime for a particular set of K and β values for which the vortices are in a stable state but not turbulent; (iii) $K_{md} < K < K^*$ where C_d increases and the effects of flow separation and vortex shedding become increasingly important, eventually leading to a very interesting half Kármán vortex street in the transverse direction in the range $8 < K < 13$† (Bearman *et al.* 1981; Bearman 1985; Sarpkaya 1985; Williamson 1985); and (iv) $K > K^*$ where C_d decreases and the number of shed vortices and flow modes increase. This last regime will not be discussed here further since it is outside the scope of the work reported herein.

According to figure 7, $K_{cr} = 1.06$, $Re_{cr} = 1097$, $K_s \approx 1.5$ and $K_t \approx 1.7$ for $\beta = 1035$. In figure 1, C_d deviates from the Stokes–Wang prediction between $K_{cr} = 0.7$ and 0.8 ($Re_{cr} = 725$ and 825). The minimum C_d in figure 1 is seen to occur at $K_{md} \approx 1.6$. Thus, it appears that the minimum drag occurs shortly after separation and when the boundary layer becomes turbulent, at least for the smooth cylinder with $\beta = 1035$. The differences between K_s, K_t, and K_{md} are too small and certainly within the limits of the experimental errors.

Figure 2 shows the same four regimes for $\beta = 1380$ with the addition of a region

† The lower limit of this range roughly corresponds to the K-value at which C_f(r.m.s.) (figure 5) breaks away from the theoretical line. Thus, $K \approx 8$ may be regarded as the upper limit of the inertia-dominated regime. Also, the inception of the transverse vortex street seems to signal the beginning of the drag-inertia-dominated regime.

of hysteresis. As K was increased in small steps (say from 0.4 to 1.5), C_d followed the Stokes–Wang line and then started to deviate from it rather rapidly between $K_{cr} = 0.7$ and 0.9 ($Re_{cr} \approx 996$–1242) (according to figure 7, $K_{cr} \approx 0.98$, $Re_{cr} \approx 1350$, $K_s \approx 1.3$ and $K_t \approx 1.55$). Subsequently C_d decreased and reached a minimum at $K_{md} = 1.5$ (note that $K_{md} \approx K_t$ as in the case of $\beta = 1035$). When K was decreased at small steps, C_d remained on the higher line, parallel to the Stokes–Wang line, and then jumped back to the laminar line at about $K = 0.55$. Despite numerous attempts it has not been possible to eliminate the hysteresis. A similar but smaller hysteresis effect was observed for the case of $\beta = 1035$ between $K = 0.6$ and 0.8. This is not shown in figure 1. The reasons for the hysteresis are neither clear nor easy to uncover, primarily due to the extreme difficulty of carrying out such experiments. It is tempting to think that for very small values of K (say $K = 0.4$) the disturbances in the flow (ambient turbulence, convection currents) are very small and the flow remains stable over a larger range of K ($K_{cr} = 0.7$ for $\beta = 1380$) which is still smaller than that indicated by figure 7. However, if the experiment is conducted by decreasing K, the turbulence generated in the boundary layers may increase the ambient turbulence in the tunnel. Even though water was kept at room temperature, the convection currents cannot be entirely discounted. The existence of real or imagined additional disturbances will tend to render the flow unstable as K is decreased gradually below 0.7 (for $\beta = 1380$). Finally, at $K = 0.55$ the flow becomes stable. It is unfortunate that one cannot be more precise, partly because the effects of wall boundary layers and ambient turbulence on the precarious nature of the vortical instability cannot be quantified and partly because it is extremely difficult to measure forces very accurately at small K-values. Probably, the time interval between the successive increments of K must be considerably increased (15 min in the present experiments) to minimize the effect of some of the disturbances.

The first instability is not evident in the data for $\beta = 11240$ (figure 3), for which the lowest K is about 0.8. Assuming that Hall's analysis can be extrapolated to $\beta = 11240$, one has $K_{cr} = 0.57$ and $Re_{cr} = 6400$. It is safe to assume that the boundary layer is already unstable and has undergone transition to turbulence at the lowest K achieved for $\beta = 11240$ (the lowest K should be about 0.2 or so to observe a transition in C_d at about $K = 0.57$ on the basis of Hall's analysis). It was not possible to conduct experiments at K-values as small as 0.2 with a large cylinder. The dry weight (as well as the buoyant force) of the cylinder required the use of larger-capacity force transducers which, in turn, made the measurement of very small forces nearly impossible. The electronic amplification of the unfiltered signals resulted in excessive noise. Since a decision was made not to filter the data, it was preferred to begin with a sufficiently high enough K value such that the noise-to-signal ratio was less than 5%.

The minimum C_d occurred at $K_{md} \approx 3.5$. It was not possible to determine K_s for $\beta = 11240$. Figure 7 shows that the transition and separation occur almost simultaneously for $\beta \approx 2600$ ($K \approx 1.25$, $Re = 3250$). For larger β, transition occurs earlier and, as noted by Bearman (1985), delays separation to a higher K. Thus, for $\beta = 11240$, separation is expected to occur at $K_s \approx 3$, using a linear extrapolation of the data shown in figure 7.

Figure 4 shows the data obtained with the rough cylinder for $\beta = 1800$. As noted earlier, the instability should begin at $K_{cr} \approx 0.4$ (probably at a smaller K on the basis of figures 1–3), a value which was unattainable in the present experiments. Apparently, the boundary layer has become unstable by the time K reaches a value of about 0.45 (lowest K in figure 4). Subsequently, C_d decreased rapidly, while remaining on a line

nearly parallel to the Stokes–Wang line, and reached its minimum value at $K_{md} \approx 2.4$. In summary, the transition at $K_t \approx 1.1$ is followed by separation at $K_s \approx 1.9$ ($Re \approx 3400$) and minimum drag at $K_{md} \approx 2.4$. Once again the delay in separation is attributed to the earlier transition in the boundary layer.

The foregoing suggests that the flow becomes unstable to axially periodic vortices at a critical value of the Keulegan–Carpenter number for a given β and k/D. The effect of roughness is to precipitate instability and transition. For smooth cylinders and for β smaller than about 2600, separation precedes transition to turbulence in the boundary layers. In this case, the minimum drag and the transition occur at about the same K. When the transition precedes separation, then the separation is delayed to a higher K-value. In this case too the minimum drag nearly corresponds to the occurrence of separation, K_s being slightly smaller than K_{md}.

Two additional observations may be made regarding the data shown in figures 1–4. First, the inertia coefficient C_m is larger than 2, at least for $K < K_t$, and nearly identical to that given by (5). The ideal values of C_m are 2.07, 2.06, 2.05, and 2.02 for $\beta = 1035$, 1380, 1800, and 11240, respectively. These values are not shown in figures 1–4 for sake of simplicity. Secondly, one cannot isolate the contribution of vortex shedding by subtracting C_d given by the Stokes–Wang analysis [see (4)] from the measured C_d since the analysis cannot account for the drag on smooth or rough cylinders with unstable or turbulent boundary layers, particularly in the range $K_{cr} < K < K_{md}$.

4. Conclusions

In-line force measurements and flow-visualization studies on smooth and rough circular cylinders have shown that (i) the theoretical values of the inertia coefficient agree quite well with those obtained experimentally for Keulegan–Carpenter numbers smaller than that corresponding to the inception of boundary-layer transition; (ii) the drag coefficient predicted by the Stokes–Wang analysis agrees well with that obtained experimentally for $K < K_{cr}$ at which the flow becomes unstable (shown only for two smooth cylinders); (iii) the critical regime is followed either by separation and transition or by transition and delayed separation. In either case, separation and minimum drag occur almost simultaneously; (iv) roughness precipitates instability (shown here for one β only) and transition to turbulence in the boundary layers. Its net effect is to increase C_d, relative to the Stokes–Wang prediction, and to delay separation; (v) Hall's analysis and Honji's conjecture that the streaked flow may form outside the range $70 < \beta < 700$ are shown to be valid for $\beta < 5500$.

The support of the National Science Foundation is gratefully acknowledged. The author would like to thank Dr P. W. Bearman and Dr D. J. Maull for stimulating discussions. He is also grateful to all the referees for a number of helpful comments. A special note of thanks is extended to Mr Jack McKay for his most skilful and dedicated work in the construction and smooth operation of the test facilities. Thanks are also due Lt. N. Q. S. Yuen for his assistance with the experiments.

REFERENCES

Bearman, P. W. 1985 Vortex trajectories in oscillating flow. In *Proc. of Separated Flow Around Marine Structures, Trondheim, Norway*, pp. 133–153. The Norwegian Institute of Technology, Trondheim, Norway.

BEARMAN, P. W., DOWNIE, M. J., GRAHAM, J. M. R. & OBASAJU, E. D. 1985 Forces on cylinders in viscous oscillatory flow at low Keulegan–Carpenter numbers. *J. Fluid Mech.* **154**, 337–356.

BEARMAN, P. W., GRAHAM, J. M. R., NAYLOR, P. & OBASAJU, E. D. 1981 The role of vortices in oscillatory flow about bluff cylinders. In *Proc. Intl Symp. on Hydrodynamics in Ocean Engng, Trondheim, Norway, August*, pp. 621–635.

HALL, P. 1984 On the stability of unsteady boundary layer on a cylinder oscillating transversely in a viscous fluid. *J. Fluid Mech.* **146**, 347–367.

HONJI, H. 1981 Streaked flow around an oscillating circular cylinder. *J. Fluid Mech.* **107**, 509–520.

KEULEGAN, G. H. & CARPENTER, L. H. 1958 Forces on cylinders and plates in an oscillating fluid. *J. Res. Nat. Bur. Standards* **60**, 423–440.

MORISON, J. R., O'BRIEN, M. P., JOHNSON, J. W. & SCHAAF, S. A. 1950 The force exerted by surface waves on piles. *Petroleum Trans.* **189**, 149–157.

ROSENHEAD, L. (ed.) 1963 *Laminar Boundary Layers*. Clarendon.

SARPKAYA, T. 1976 Vortex shedding and resistance in harmonic flow about smooth and rough circular cylinders at high Reynolds numbers. *Tech. Rep. No.* NPS-59SL76021, Naval Postgraduate School, Monterey, CA.

SARPKAYA, T. 1977 In-line and transverse forces on cylinders in oscillatory flow at High Reynolds numbers. *J. Ship Res.* **21**, 200–216.

SARPKAYA, T. 1985 Past progress and outstanding problems in time-dependent flows about ocean structures. In *Proc. of Separated Flow Around Marine Structures, Trondheim, Norway*, pp. 1–36. The Norwegian Institute of Technology, Trondheim, Norway.

SARPKAYA, T. & ISAACSON, M. 1981 *Mechanics of Wave Forces on Offshore Structures*. New York: Van Nostrand Reinhold.

STOKES, G. G. 1851 On the effect of the internal friction of fluids on the motion of pendulums. *Trans. Camb. Phil. Soc.* **9**, 8–106.

WANG, C.-Y. 1968 On high-frequency oscillating viscous flows. *J. Fluid Mech.* **32**, 55–68.

WILLIAMSON, C. H. K. 1985 Sinusoidal flow relative to circular cylinders. *J. Fluid Mech.* **155**, 141–174.